Magnetoconductance of quasicrystals and their approximants: A study of quantum interference effects

P. Lindqvist,* P. Lanco, and C. Berger

Laboratoire d'Etudes des Propriétés Electroniques des Solides, Centre National de la Recherche Scientifique, Boîte Postale 166X, 38042 Grenoble Cedex 9, France

A. G. M. Jansen

Hochfeld Labor, Max Planck Institut, Boîte Postale 166X, 38042 Grenoble Cedex 9, France

F. Cyrot-Lackmann

Laboratoire d'Etudes des Propriétés Electroniques des Solides, Centre National de la Recherche Scientifique, Boîte Postale 166X, 38042 Grenoble Cedex 9, France

The magnetoconductance $\Delta\sigma(B)$ of a series of high-quality quasicrystals and approximants is discussed in terms of quantum interference effects. The $\Delta\sigma(B)$ data cover a wide temperature range from 0.1 to 200 K and magnetic fields as high as 20 T. Strong electron interactions are found, through inelastic electron-electron scattering as the main inelastic-electron-scattering mechanism and an enhanced electron screening. Evidence for a suppression of the quantum interference effects close to the metal-insulator transition in quasicrystals are discussed.

I. INTRODUCTION

The thermodynamically stable quasicrystals (QC) in the AlCu(Fe,Ru,Os) (Ref. 1) and AlPd(Mn,Re) (Ref. 2) systems show a structural ordering equally as well defined as in good crystalline systems.[3] This is in contrast to metastable quasicrystalline systems like AlMn or even stable ones like Ga-Mg-Zn and Al-Cu-Li, where the interior structural disorder is found to be much larger. The difference between these two groups of QC comes through in the observed electronic-transport properties.[4] The electrical conductivity σ and its temperature dependence $\sigma(T)$ in the less ordered QC are comparable to the ones for most amorphous metals, i.e., $\sigma > 1000$ $(\Omega$ cm$)^{-1}$, and the increase in σ between 4 and 300 K is of the order a few percent. The well-ordered QC show much lower σ's, in the range 1–300 $(\Omega$ cm$)^{-1}$ at 4 K and the temperature dependence is remarkably strong with $1.5 \le \sigma(300$ K$)/\sigma(4.2$ K$) \le 28$.[4–9] These values are comparable to doped semiconductors, but as must be emphasized, the controlling transport mechanism is markedly different. First, the $\sigma(T)$ cannot be interpreted in terms of a simple activation process over an energy gap or by a standard hopping process.[10] Second, as found by specific heat and x-ray-photoemission spectroscopy measurements,[4,6,11,13] the electronic density of states $(N(0))$ is of the same magnitude as in a metal, but reduced by roughly one-third below the free-electron value. Also, other transport properties like the Hall effect and the thermoelectric power show very anomalous behaviors for a metal.[4] There is thus a need for alternative mechanisms for explaining electronic transport in QC.

Indeed, since the QC have no periodic order, the usual Bloch wave formalism with all its implications is not applicable. The so-called approximants are thus of special interest. Approximants possess strong structural similarities with the QC when local order is considered,[12] but can be described by a unit cell and translation symmetries. The unit cells are large and may contain several hundreds of atoms. Calculations of the band structure on model systems of approximants reveal a complicated structure with many flat bands close to the Fermi level.[13] The best known approximants from the point of view of measurements of transport properties are the rhombohedral Al-Cu-Fe ($\frac{3}{2}$ approximant, $a \approx 32$ Å, > 600 atoms/unit cell) and cubic α-Al-Mn-Si (1/1 approximant, $a = 12.68$ Å, 138 atoms/unit cell[14]), both exhibit a conductivity value and a $\sigma(T)$ similar to the well-ordered QC.[4,15–18] This implies that the mean range structural order, which is over lengths of the size of a unit cell, is the main structural feature controlling the electron transport.

A different type of hopping electronic motion between structural entities has been suggested on this length scale ~ 10–20 Å. The idea was supported by the finding of a different type of electron states by numerical studies on quasiperiodic (or approximant) tilings.[13] These states are neither extended nor localized; they are called critical. They have an electron wave envelope that decays as a power law when compared to localized states where it decays exponentially. The interesting point for our purpose here is that the electronic propagation may become diffusive at large scale even with such peculiar states.

Going back to the $\sigma(T)$ and its magnetic-field dependence $\sigma(T,B)$ at low temperatures, there is a consensus[7,19–22] in favor for quantum interference (QI) effects in QC.[23,24] This at first seems surprising considering that QC like Al-Cu-Fe and Al-Pd-Mn are structurally well ordered and that QI phenomenon are generally associated with disorder. Quantum interference effects

     <u>51</u>   4796

are found to be present in very different metallic systems like doped semiconductors, metal-oxide-semiconductor field-effect transistor thin metal films, and metallic glasses. Actually, the one and only common feature that the QI effects require is that the coherence length of the electron wave is much longer than that of the electron mean free path. A short mean free path is usually associated with a small diffusion constant (D), and the well-ordered QC are all found to have very small D. In this context, it is not surprising that QI effect are also present in QC. The two main QI effects are the weak localization (WL) and the electron-electron interaction (EEI) effects. A simplification of the two phenomena enables us to see the WL and EEI effects as corrections to electronic properties through a correction in D or $N(0)$, respectively. In principle, the theory makes it possible to determine microscopic properties of the electrons such as the inelastic and spin-orbit scattering times, and effective electron interaction constants. These quantities give necessary information for testing electron propagation models.

The purpose of this paper is to give a general description of the magnetoconductance $\Delta\sigma(B)$ of the well-ordered three-dimensional QC and their approximants in the framework of QI effects. The samples studied cover several systems such as icosahedral (i) Al-Cu-Fe, Al-Pd-Mn and Al-Pd-Re QC, and the approximants rhombohedral (R) Al-Cu-Fe and cubic α–Al-Mn-Si. The $\Delta\sigma(B)$ has been measured over a wide temperature range, from 0.1 to 200 K and in continuous magnetic fields up to as high as 20 T. As far as we know, this temperature range is much larger than in any previous work of QI in the magnetoresistance. In QC the QI effects are about 100 times larger than in the metallic glasses, which makes it possible to measure $\Delta\sigma$ at high temperature (over about 50 K). Despite this large $\Delta\sigma$ (several percent or even more) and the low σ of the samples, the QI theory used on QC seems to work well.[17,19–22] Here, we want to point out the similarities in different QC and approximants and make a comparison with amorphous metals. We also discuss the basis for how various fits have been made (question of input parameters, fitting temperature and field ranges) and how well we can trust the parameters extracted from the QI theory for the large $\Delta\sigma$ observed. In the fitting procedures we discuss, the standard procedure of fitting all data directly to theory was avoided. The merit of our methods is that the different features observed are directly visualized and can be compared, even though parameters from theory were not well determined. Actually, our rigorous approach in the fitting procedure gives us a large range for the parameters obtained from theory. This data treatment goes beyond previous works where it has been proved that magnetoresistance can be fitted by the QI theory, but where the obtained parameters are effective only from examples of such fits. The power p in the temperature dependence of $\tau_{ie} \sim T^{-p}$ and the electron screening parameter F_σ are well determined, while the absolute values of the inelastic and spin-orbit scattering times, $\tau_{ie}(T)$ and τ_{so} respectively, remain uncertain. However, the results give a complete description of QC and their approximants.

II. QUANTUM INTERFERENCE EFFECTS

The QI theories describe corrections to the electronic-transport properties through weak localization (WL) (Ref. 25) and electron-electron interaction (EEI) (Refs. 26–28) effects. Considering small corrections from QI, we write the total temperature (T) dependence of σ as

$$\sigma(T) = \sigma_B(T) + \sigma_{WL}(\tau_{ie}(T), \tau_{so}, D'_{WL})$$
$$+ \sigma_{EEI}(T, D'_{EEI}, F_\sigma) , \qquad (1)$$

and the corresponding magnetic-field (B) dependence as

$$\Delta\sigma(B) = \Delta\sigma_B(B) + \Delta\sigma_{WL}(\tau_{ie}(T), \tau_{so}, D'_{WL}, g^*, B)$$
$$+ \Delta\sigma_{EEI}(T, D'_{EEI}, F_\sigma, g^*, B) , \qquad (2)$$

where $\tau_{ie}(T)$ and τ_{so} are the inelastic and spin-orbit scattering times of the electrons, respectively. g^* is the effective Landé g factor, and F_σ is an electron screening constant. The D'_{WL} and D'_{EEI} are the electronic diffusion constants used in the WL and EEI parts, respectively. Their relation to the electronic diffusion constant deduced from the electronic specific heat (D_{Exp}) will be discussed later. We consider here only the EEI contributions in $\sigma(T)$ and $\Delta\sigma(B)$ from the particle-hole channel, since the ones from the particle-particle channel are of much smaller magnitude for a nonmagnetic or nonsuperconducting material and can be neglected.[23] The $\sigma_B(T)$ and $\Delta\sigma(B)$ formally stand for the Boltzmann contributions, but they can stand for all other possible conduction mechanisms.

We now give a short description with expressions for the different QI terms in Eqs. (1) and (2) in three dimensions. The $\sigma_{WL}(T)$ gives a negative contribution and its T dependence $\Delta\sigma_{WL}(T)$, $\sigma(T) = \sigma_{WL}(0) + \Delta\sigma_{WL}(T)$, is given by[25]

$$\Delta\sigma_{WL}(T) = A[3\sqrt{t+1} - \sqrt{t}] , \qquad (3)$$

where

$$A = \frac{e^2}{2\pi^2\hbar\sqrt{D\tau_{so}}} \qquad (4)$$

and

$$t = \tau_{so}/4\tau_{ie}(T) . \qquad (5)$$

The $\Delta\sigma_{WL}(T)$ has a minimum for $\tau_{so}/\tau_{ie}(T) = \frac{1}{2}$. The T-dependence part of $\sigma_{EEI}(T)$ is positive or negative depending on the size of F_σ and is proportional to $\sqrt{T}$. We have $\Delta\sigma_{EEI}(T)$ (Ref. 23),

$$\Delta\sigma_{EEI}(T) = \frac{e^2}{4\pi^2\hbar} \frac{1.3}{\sqrt{2}} \left[\frac{3}{2}F_\sigma - \frac{4}{3} \right] \left[\frac{k_B T}{\hbar D} \right]^{1/2} . \qquad (6)$$

In the limit of high temperatures, both contributions vanish, i.e., $\sigma_{WL}(T) = \sigma_{EEI}(T) = 0$.

The magnetic-field influence on WL including spin splitting is given by[25]

$$\frac{\Delta\sigma_{WL}(B)}{A} = \sqrt{h} f_3 \left[\frac{1+t}{h} \right]$$

$$+ \frac{1}{2} \frac{\sqrt{h}}{\sqrt{1-\gamma}} \left[f_3 \left[\frac{t_+}{h} \right] - f_3 \left[\frac{t_-}{h} \right] \right]$$

$$- \frac{(\sqrt{t} - \sqrt{t_+})}{\sqrt{1-\gamma}} - \sqrt{t+1} + \sqrt{t} , \quad (7)$$

where

$$h = \frac{eDB\tau_{so}}{\hbar} , \quad (8)$$

$$\gamma = \left[\frac{g^* \mu_B h}{2eD} \right]^2 , \quad (9)$$

$$t_\pm = t + 0.5(1 \pm \sqrt{1-\gamma}) , \quad (10)$$

the f_3 function has the limiting values,

$$f_3(x) = \begin{cases} 0.6094 & \text{when } x = 0 \\ \dfrac{x^{-3/2}}{48} & \text{when } x \gg 1 \end{cases} \quad (11)$$

and, A and t are given by Eqs. (4) and (5), respectively. Without spin splitting (set $\gamma = 0$), the $\Delta\sigma_{WL}(B)$ is negative when $\tau_{so} \ll \tau_{ie}(T)$, positive when $\tau_{so} > \tau_{ie}(T)$, and always positive in the limit of very high fields. The spin splitting in WL, mainly the last four square-root terms in Eq. (7), gives a negative contribution which saturates at high fields. The spin splitting is only of importance for systems with $D < 1$ cm^2/s.[29] For EEI, we have the magnetic-field dependence[28]

$$\Delta\sigma_{EEI}(B) = -F_\sigma \frac{e^2}{4\pi^2\hbar} \left[\frac{k_B T}{2\hbar D} \right]^{1/2} g_3 \left[\frac{g^* \mu_B B}{k_B T} \right] , \quad (12)$$

and

$$g_3(x) = \begin{cases} 1.900 - 2.294\sqrt{x} & \text{if } x \gg 1 \\ 0.329 x^{3/2} & \text{if } x \ll 1. \end{cases} \quad (13)$$

The $\Delta\sigma_{EEI}(B)$ is negative, since $F_\sigma > 0$. For $f_3(x)$ and $g_3(x)$, we used the standard series expansion expressions.[30] The field dependence for both effects start as B^2 for "low" field. At "high" field the EEI part gives a $\sqrt{B}$ dependence, while WL may give a $\sqrt{B}$ or weaker dependence. The magnetic-field effects disappear as well with increasing T. In this paper, we use the words "low" and "high" fields for when we observe a B^2 dependence or not. Thus at high temperatures, we are in the "low-" field limit even if the magnetic field reaches 20 T.

The usual procedure is now to set $\Delta\sigma_B(B) = 0$ and $\sigma_B(T) = \sigma_B(0)$. The former can be justified since the classic magnetoconductance is obeying Kohlers rule which is a function of σB, and this is a small quantity. The latter is not so evident when the temperature exceeds 10 or 20 K. Also, we know that the EEI contribution should start to deviate from the $\sqrt{T}$ law of $\sigma_{EEI}(T)$ and disappear at temperatures of about 10 to 50 K,[29,31] while

the WL effect may be present at higher temperatures. The limiting factor for when WL disappears is $\tau_{ie}(T) \approx \tau$, where τ is the elastic-scattering time, but when this happens, it is now known. Thus, a fitting of the temperature dependence $\sigma(T)$ can give quite uncertain parameters, while the magnetoconductance is a much better quantity for determining parameters.

In the past few years, there has been some analyses, for i-Al-Cu-Fe by Haberkern, Fritsch, and Schilling[19] and by Sahnoune, Ström-Olsen, and Zaluska,[20] but some of the most pressing problems have not been discussed. We now discuss four of them. First, the experimentally observed magnetoconductance $\Delta\sigma_{Exp}(B)$ is of the order of 1–30 %, while the theory is a perturbation calculation assuming the individual contributions are small and independent, and hence assumed to be simply additive. Strictly for this, we require $k_F l \gg 1$. In a nearly free-electron model, we have $k_F l = 3m^* D/\hbar$, which gives $k_F l = 0.26(m^*/m_e)$ for a QC typical value of $D = 0.1$ cm^2/s. The m^* and m_e denote the effective and free-electron masses, respectively. One may, thus, ask if the QI theory can be used as it is. This is a serious question which has to be kept in mind. However, we have a similar situation in the case of metallic glasses, where D is in the range 0.3 to 3 cm^2/s, and the theory seems to work equally well as for QC. It could also be questioned if the additivity of the WL and EEI contribution, which is the basic idea of Eqs. (1) and (2), still holds in the case of large magnetoconductance values. Since a complete theory, which takes all contributions of arbitrary size simultaneously into account, is not available, we assume the present one is correct.

Second, for fitting the unknown $\tau_{ie}(T)$, τ_{so}, g^*, and F_σ we need first of all D, but the problem is now as follows: what are the values of D'_{WL} and D'_{EEI}? In systems where the QI effects are small, one may set $D'_{WL} = D'_{EEI} = D_{Exp}$ and independent of T. D_{Exp} is an experimentally determined diffusion constant. However, this cannot be true in our case. Equations (1) and (2) assume that the different contributions are independent. Therefore, as a first approximation, we should use input parameters where the effect itself, WL or EEI, is not included. D_{Exp} is calculated from the specific heat γ at $T = 0$ and $\sigma_{Exp}(T)$ using the relations $\gamma = (\pi k_B)^2 N(0)/3$ and $\sigma_{Exp}(T) = e^2 N(0) D_{Exp}(T)$. The EEI effect is present in $N(0)$ too, which gives $N_{Exp}(0) = N_B(0) + N_{EEI}(0)$, and $\sigma_{Exp}(T)$ is given by Eq. (1). We have

$$D'_{EEI}(T) = [\sigma_{Exp}(T) - \sigma_{EEI}(T)]/e^2[N_{Exp}(0) - N_{EEI}(0)]$$

$$\approx \sigma_{Exp}(T)/e^2 N_{Exp}(0) = D_{Exp}(T) \quad (14)$$

and

$$D'_{WL}(T) = [\sigma_{Exp}(T) - \sigma_{WL}(T)]/e^2 N_{Exp}(0) > D_{Exp}(T) . \quad (15)$$

In Eq. (14), we use $[1 - \sigma_{EEI}(T)/\sigma_{Exp}(T)]/[1 - N_{EEI}(0)/N_{Exp}(0)] \approx 1$. This is true when the EEI terms are at most some 10% of the experimental values. To obtain D'_{WL} the problem is to estimate the WL part in

$\sigma_{Exp}(T)$. As will be shown later, WL is present with a large magnitude when $T < 50$ K. We assume the total change in $\sigma_{Exp}(T)$ below 100 K as a lower limit for $\sigma_{WL}(T)$, which gives $D_{Exp}(100$ K$)$. An upper limit is more difficult to specify, but cannot be much higher than the total change up to room temperature. For simplicity the D's were taken temperature independent in the proceeding analyses with $D_{Exp}(100$ K$) \leq D'_{WL} \leq D_{Exp}(300$ K$)$ and $D'_{EEI} = D_{Exp}(4.2$ K$)$.

Third, often $\Delta\sigma(B, T_M)/\sigma(0, T_M)$ instead of $\Delta\sigma(B, T_M)$ is fitted. Here T_M is the temperature at which the magnetoconductance is measured. This is usually done since $\Delta\sigma(B, T_M)/\sigma(0, T_M)$ is a quantity better known than $\Delta\sigma(B, T_M)$, but it only moves the uncertainty from the fitted data to a σ parameter which enters the fitted expression. As long as $\sigma(T)$ varies only a few percent in the T range studied this can be allowed, but if the variation is larger the renormalization should be $\Delta\sigma(B)/\sigma' = [\Delta\sigma(B, T_M)/\sigma(0, T_M)][\sigma(T_M)/\sigma(T_{Ref})]$, where T_{Ref} is a reference temperature. The value of $\sigma(T_{Ref})$ enters now in the expressions above. In our case, the fitting with T_{ref} only introduce a change of a few percent in the parameter, so $\Delta\sigma(B, T_M)/\sigma(0, T_M)$ was used for convenience. More serious is the use of $\Delta\rho(B)/\rho$ when $\Delta\sigma(B)/\sigma \geq 10\%$. In this case, we are not allowed to set $\Delta\rho(B)/\rho = -\Delta\sigma(B)/\sigma$ for the theoretical contributions. Examining the works on QI in QC, this last point seems to have been neglected.

The latest remark concerns the value of the effective g factor g^*. We have $g^* = 2$ for free electrons. This value can be smaller or larger due to scaling with the effective mass and should be normalized with the Stoner enhancement factor.[32] The latter effect must, however, be small since QC are diamagnetic at higher temperature. A very weak paramagnetic contribution, implying less than ~ 50 ppm impurity spins, is often present at low T.[8,33,34] We will not include magnetic scattering contributions in the analysis, but their influence will be discussed later.

III. EXPERIMENTAL RESULTS AND ANALYSIS

A. Experiment

The sample preparations are described here only briefly.[6,8,35] High-purity materials were melted into in-

gots of nominal compositions and then melt spun into ribbons or splat quenched to flakes. A heat treatment in evacuated silica ampoules produced single phase material of the desired phase. The i-Al$_{62}$Cu$_{25.5}$Fe$_{12.5}$ and i-Al$_{62.5}$Cu$_{25}$Fe$_{12.5}$ alloys were heat treated at 1073 K for 3 h, the R-Al$_{62.8}$Cu$_{26}$Fe$_{11.2}$ was obtained after 11 days at 973 K, and with a subsequent treatment at 993 K for three days for transforming it to the i phase. The i-Al$_{70.5}$Pd$_{22}$Mn$_{7.5}$ and i-Al$_{70.5}$Pd$_{22}$Re$_{7.5}$ alloys were annealed at 1023 K for 24 h, and α-Al$_{72.5}$Mn$_{17.4}$Si$_{10.1}$ at 883 K for three days. X-ray diffraction was used to verify the structure. No trace of supplementary phases was found.

The magnetoconductivity was measured at Centre National des Champs Intenses—Max Planck Institut (SNCI-MPI) high-field facility in three series of measurements by standard four-probe methods in the temperature range 0.1 to 200 K, as follows: (a) In a dilution refrigerator between 0.1 and 1 K, (b) in a He^3 cryostat between 0.4 and 4.2 K, and (c) in a He^4 flow cryostat between 4.2 and 200 K. The samples studied were i-Al$_{62.5}$Cu$_{25}$Fe$_{12.5}$: (c); i-Al$_{62}$Cu$_{25.5}$Fe$_{12.5}$: (a) and (c); i-Al$_{62.8}$Cu$_{26}$Fe$_{11.2}$: (b) and (c); R-Al$_{62.8}$Cu$_{26}$Fe$_{11.2}$: (b) and (c); i-Al$_{70.5}$Pd$_{22}$Mn$_{7.5}$: (b) and (c); i-Al$_{70.5}$Pd$_{22}$Re$_{7.5}$: (b); and α-Al$_{72.5}$Mn$_{17.4}$Si$_{10.1}$: (b) and (c). Permanent magnetic fields up to 20 T were used, except in (a) where it was 10 T. Above temperatures of about 30 K the magnetic-field dependence of the resistance temperature sensors start to become critical. A magnetic field independent capacitance sensor was used for controlling T at these temperatures and a Pt-100 resistor to monitor the slow drift in T of a few 100 mK during a sweep up and down in field. The conductance values of the samples were later corrected for this drift by using tabulated values of the magnetoresistance of Pt thermometers[36] adjusted to fit our Pt sensor. In this way, a relative temperature error of ± 30 mK was obtained at the highest temperatures (200 K). Typically, a few hundred points were measured for each field sweep at low temperatures and around 50 for high temperatures.

B. Magnetoconductance: General trends

The $\sigma(4.2$ K$)$ values and the $\sigma(300$ K$)/\sigma(4.2$ K$)$ ratio of the samples are tabulated in Table I. The error in σ is about $\pm 10\%$. We note that the values for the i- and the

TABLE I. Sample properties and fitted parameters for some quasicrystals and approximants.

Sample	$\sigma(4.2$ K$)$ [$1/\Omega$ cm]	$\sigma(300$ K$)/\sigma(4.2$ K$)$ [$-$]	$D(4.2$ K$)_{Exp}$[a] [cm^2/s]	$\Delta\sigma(0.6$ K, 10 T$)$ [$1/\Omega$ cm]	$T_{\Delta\sigma(B)=0}$ [K]	p [$-$]	$F_{\sigma-max}$[b] [$-$]	g^*[b] [$-$]
i-Al$_{62.5}$Cu$_{25}$Fe$_{12.5}$:	95	2.45	0.075		100			
i-Al$_{62}$Cu$_{25.5}$Fe$_{12.5}$:	130	2.15	0.095	-20.5		1.45 ± 0.4	1.5 ± 0.2	$1.7^{+2}_{-0.7}$
i-Al$_{62.8}$Cu$_{26}$Fe$_{11.2}$:	210	1.75	0.16	-10.6	120	1.4 ± 0.4	0.7 ± 0.2	$1.7^{+6}_{-0.7}$
R-Al$_{62.8}$Cu$_{26}$Fe$_{11.2}$:	220	1.68	0.16	-10.1	100	1.15 ± 0.35	0.7 ± 0.2	$2.1^{+6}_{-0.6}$
i-Al$_{70.5}$Pd$_{22}$Mn$_{7.5}$:	100	2.25	0.055	-18.0	170	1.3 ± 0.4	0.75 ± 0.2	$3.0^{+5}_{-1.3}$
i-Al$_{70.5}$Pd$_{22}$Re$_{7.5}$:	50	4	0.055	-9.3			0.95 ± 0.05	$1.3^{+0.3}_{-0.2}$
α-Al$_{72.5}$Mn$_{17.4}$Si$_{10.1}$:	235	2.75	0.10	-19.9	160	1.0 ± 0.3	1.10 ± 0.25	$0.9^{+1}_{-0.4}$

[a]The diffusion constants are calculated from specific-heat measurements (Refs. 4–6 and 52) as described in the text.
[b]The error limits are defined as when the root-mean-square value for the fit is doubled.

P. LINDQVIST *et al.*

crystalline R-Al$_{62.8}$Cu$_{26}$Fe$_{11.2}$ are almost identical. Note that due to errors in the geometrical factors for determining $\sigma(4.2$ K), it is difficult to say whether the i and R phases display identical or only similar behaviors. The $\sigma(300$ K)/$\sigma(4.2$ K) ratio gives a better indication, since this ratio is generally correlated with the inverse of $\sigma(4.2$ K) within a system. Both $\sigma(4.2$ K) and $\sigma(300$ K)/$\sigma(4.2$ K) give strong evidence that electron transport properties are mainly determined by the local order. For the α–Al-Mn-Si approximant the values are comparable to those for the i- and R-Al$_{62.8}$Cu$_{26}$Fe$_{11.2}$. The other Al-Cu-Fe and the Al-Pd-Mn samples correspond to materials with the lowest σ in respective system.[8,37]

The measured $\Delta\sigma(B)/\sigma$ curves will now be described an discussed by referring to the QI formulas. In Figs. 1(a)–1(d), we show $\Delta\sigma(B)/\sigma$ for i-Al$_{62.8}$Cu$_{26}$Fe$_{11.2}$, R-Al$_{62.8}$Cu$_{26}$Fe$_{11.2}$, i-Al$_{70.5}$Pd$_{22}$Re$_{7.5}$ and i-Al$_{62}$Cu$_{25.5}$Fe$_{12.5}$ at low T, and in Figs. 2(a)–2(c), we follow $\Delta\sigma(B)/\sigma$ for i-Al$_{70.5}$Pd$_{22}$Mn$_{7.5}$ from 0.4 to 194 K. The $\Delta\sigma(B)/\sigma$ is negative for all samples and most temperatures and it is approximately linear in $\sqrt{B}$ as predicted by the QI theory. However, there is a tendency for deviations from $\sqrt{B}$ at high fields, which is very pronounced for Al-Pd-

Re [see Fig. 1(c)]. The T dependence of $\Delta\sigma(B)/\sigma$ is fairly strong at the lowest T. This is an indication of a large EEI contribution, since the value of the g_3 function in the EEI is only large when $B/T \gg 1$ [see Eqs. (12) and (13)] and the WL is usually saturated.[38-40] At around 10 K, the EEI effect is small, thus a remaining large magneto-conductance is due to WL. Here, all the samples display a negative $\Delta\sigma(B)/\sigma$, which is typical for a strong spin-orbit scattering system, i.e., $\tau_{ie}(T) > \tau_{so}$ over most T. As the temperature increases, we observe $\Delta\sigma(B)/\sigma$ decrease, and above about 50 K only $\Delta\sigma(B) \sim B^2$ is found, which is the "low-" field dependence [see Fig. 2(b)–2(c)]. A change of sign is also observed around 100 to 200 K. This is expected when $\tau_{ie} \ll \tau_{so}$ [see also Figs. 4(a)–4(c)]. Thus, all main features observed are expected within the QI theory. Concerning the magnitude of the effects, the Figs. 1 and 2 clearly display the large values of $\Delta\sigma(B)/\sigma$. The maximum values for $\Delta\sigma(B)$ range from 7% to 30%, with generally a larger variation for a lower σ. In Table I, we also give the absolute values of $\Delta\sigma(B)$ at low T for an arbitrary chosen T and B reference value. As seen the absolute values differs much less, but do not correlate with σ or $D_{Exp}(4.2$ K).
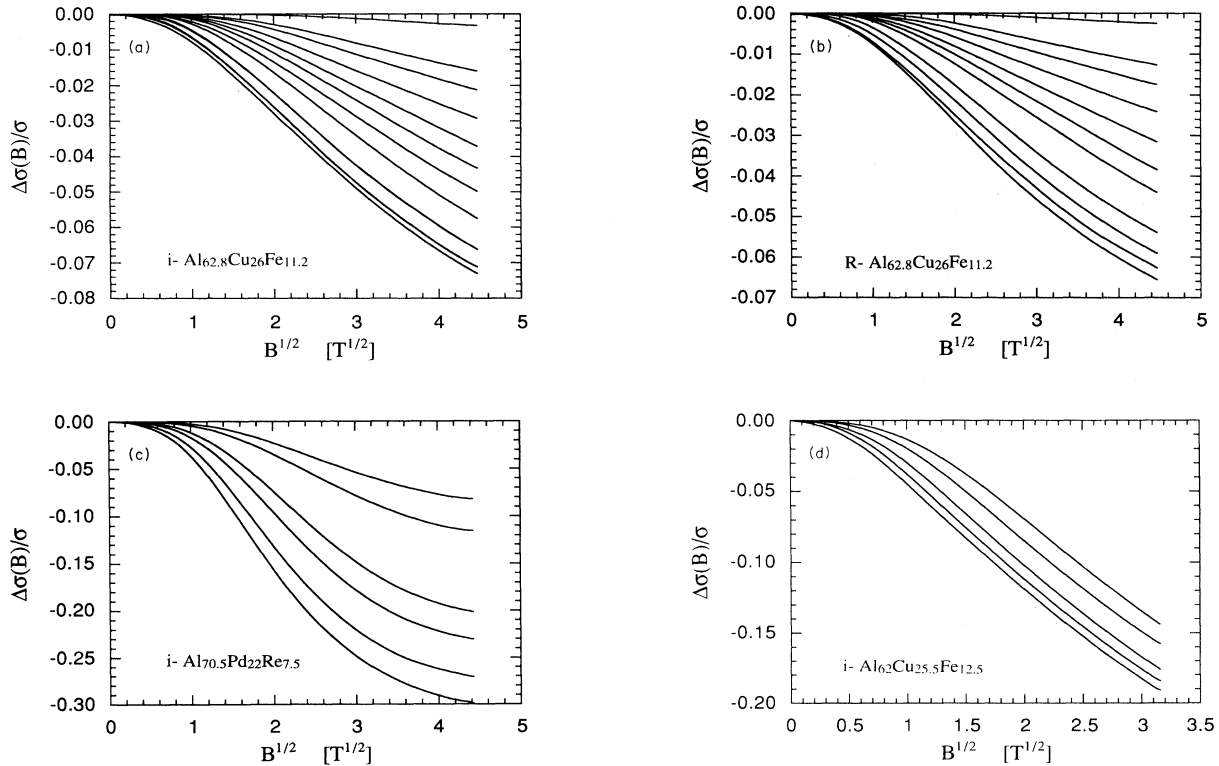
FIG. 1. (a) The $\Delta\sigma(B)/\sigma$ vs $\sqrt{B}$ for i-Al$_{62.8}$Cu$_{26}$Fe$_{11.2}$. Temperatures for the curves are, from the bottom 0.4, 0.6, 1.0, 2.2, 3.1, 4.2, 6, 8, 12, 16, and 34 K. These $\Delta\sigma(B)/\sigma$ are to be compared with the R phase for corresponding composition. In $\Delta\sigma(B)$ they are identical (see Table I), indicating that the microscopic properties in the QI theory are the same. (b) The $\Delta\sigma(B)/\sigma$ vs $\sqrt{B}$ for R-Al$_{62.8}$Cu$_{26}$Fe$_{11.2}$. Temperatures for the curves are, from the bottom, 0.4, 0.6, 1.0, 1.6, 3.1, 4.2, 6, 8, 12, 16, and 35 K. (c) The $\Delta\sigma(B)/\sigma$ vs $\sqrt{B}$ for i-Al$_{70.5}$Pd$_{22}$Re$_{7.5}$. Temperatures for the curves are, from the bottom, 0.40, 0.63, 1.0, 1.4, 3.1, and 4.2 K. (d) The $\Delta\sigma(B)/\sigma$ vs $\sqrt{B}$ for i-Al$_{62}$Cu$_{25.5}$Fe$_{12.5}$. Temperatures for the curves are, from the bottom, 0.09, 0.22, 0.33, 0.59, and 0.90 K.
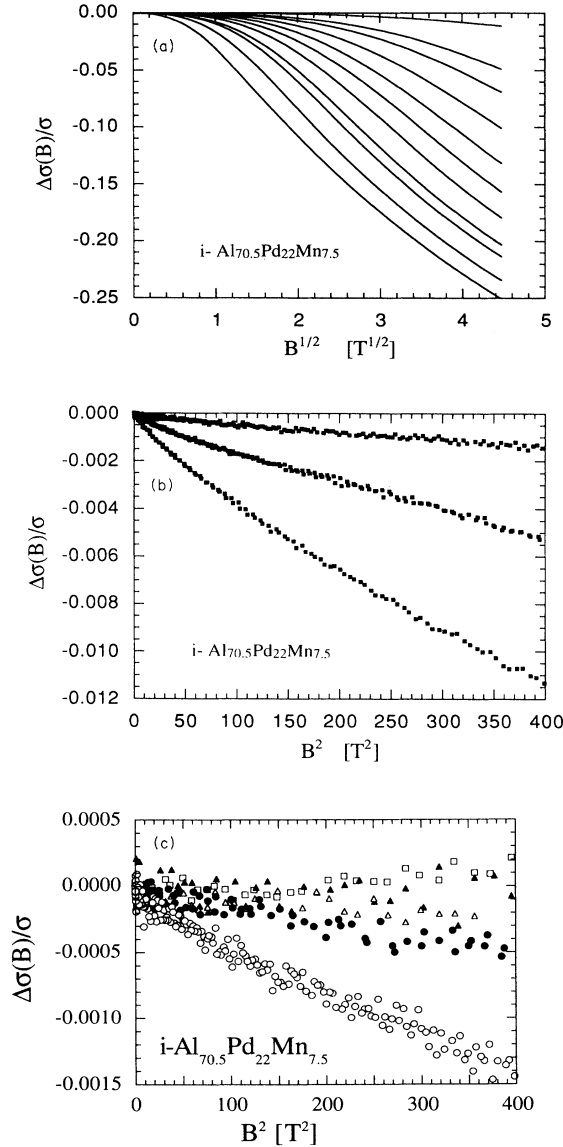
FIG. 2. (a) The $\Delta\sigma(B)/\sigma$ vs $\sqrt{B}$ for i-Al$_{70.5}$Pd$_{22}$Mn$_{7.5}$. Temperatures are, from the bottom, 0.4, 1.0, 1.6, 2.2, 3.1, 4.2, 6, 8, 12, 16, and 35 K. (b) The $\Delta\sigma(B)/\sigma$ vs B^2 for i-Al$_{70.5}$Pd$_{22}$Mn$_{7.5}$. Temperatures are, from the bottom, 35, 54, and 85 K. (c) The $\Delta\sigma(B)/\sigma$ vs B^2 for i-Al$_{70.5}$Pd$_{22}$Mn$_{7.5}$. Temperatures are 85 K, $\circ$; 116 K, $\bullet$; 133 K, $\triangle$; 160 K, $\blacktriangle$; and 194 K, $\square$.

C. Fitting parameters

Problems related to input parameters in the QI theories have been discussed in a previous section, where we found $D'_{EEI} = D_{Exp}(4.2$ K$)$ and $D_{Exp}(100$ K$)$ $\leq D'_{WL} \leq D_{Exp}(300$ K$)$. To calculate the D_{Exp}, we need the specific heat γ. As we cannot find data for the exact compositions of all our samples, we have assumed γ to be concentration independent in each system. From data in the literature, this is true for Al-Cu-Fe, but not for Al-Cu-Ru measured in a wider compositional range. In Al-

Cu-Fe, $N(0)$ (Refs. 3 and 6) is found roughly independent of composition, while σ changes at least by a factor of two. In contrast to this, for Al-Cu-Ru there is a dependence of σ on $N(0)$, which is not linear.[15] Different approaches have been used previously to solve this problem. For example, Sahnoune, Ström-Olsen, and Zaluska assumed d to be constant in the Al-Cu-Fe system,[20] which we know now to be incorrect, while Haberkern, Fritsch, and Schilling fitted it.[19] However, the difference between D'_{WL} and D'_{EEI} has been neglected. In Table I, $D_{Exp}(4.2$ K$)$ which was used in the fits is presented. For g^* the free-electron value, $g^* = 2$, is frequently used, but we prefer to fit it, since the actual value may deviate considerably from $g^* = 2$. Finally, we have the three standard fit parameters τ_{ie}, τ_{so}, and F_σ.

One may now object, D'_{EEI}, D'_{WL}, and g^* can be fitted together with $\tau_{ie}(T)$, τ_{so}, and F_σ. The magnetoconductance curves are, however, simple functions of B and can be fitted by many sets of parameters. The best fits are usually not as good as the measurement quantities, which expand even more the allowed parameter range. The latter depends on the relative size of the individual contributions as well. We have fitted the full theory to all data, but here we will present and study only two different limits which allows us to fit the EEI and WL effects almost independent by each other.[38] The advantage is that the individual effects can be visualized, while direct fits have a tendency to hide the physical manifestations of the different contributions behind values. Also, an uncertainty in input parameters results in an uncertainty in the output parameters, which is avoided here.

D. Analysis

In amorphous metals, a saturation or a weak T dependence of the WL contribution is found below a few Kelvin.[38,39] A justification for this to be valid also for QC is given later. This allows us to separate the EEI part in $\Delta\sigma(B)/\sigma$ by plotting the difference $\Delta\sigma(B,T)/\sigma(0,T)$-$\Delta\sigma(B,T_{Ref})/\sigma(0,T_{Ref})$, with T fixed for each $\Delta\sigma(B)/\sigma$ curve and to fit the quantity to theory with only two parameters. The reference temperature T_{Ref} is taken when the WL is thought to be saturated, around $1-1.5$ K, and F_σ and g^* are evaluated with only the EEI expression. This gives the maximum values $F_{\sigma\text{-max}}$. An example of such a treatment for i-Al$_{62}$Cu$_{25.5}$Fe$_{12.5}$ with $T_{Ref} = 0.9$ K is given in Fig. 3. Points are calculated from measurement data, and lines are the best fits with $F_{\sigma\text{-max}} = 1.5$ and $g^* = 1.7$. Since this is a fit of only two parameters, the agreement between theory and experiment is astonishingly good. The experimental data are parallel and approximately constant at high fields. The same behaviors are found in all the other samples, including Al-Pd-Re. Thus the observed deviation from $\sqrt{B}$ for Al-Pd-Re in Fig. 1(c) is due to WL. Fitted values can be found in Table I. It is of course possible to improve the fits by including the WL effect too, but this increases the number of fit parameters from two to five, and enlarges the error bars of individual parameters. Such a treatment reduces F_σ by typically 50% and depends strongly on the size of $\Delta\sigma(B,T)/\sigma(0,T)$-$\Delta\sigma(B,T_{Ref})/\sigma(0,T_{Ref})$. For instance
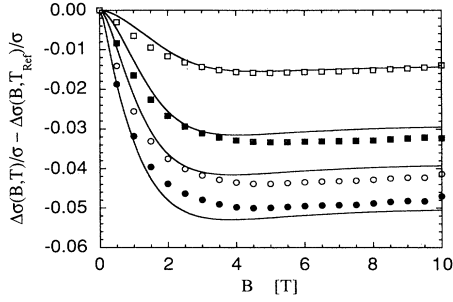
FIG. 3. The $\Delta\sigma(B,T)/\sigma - \Delta\sigma(B,T_{Ref})/\sigma$ vs $\sqrt{B}$ for i-$Al_{62}Cu_{25.5}Fe_{12.5}$. $T_{Ref}=0.9$ K. The solid lines are fits to theory as described in the text with $F_\sigma=1.5$ and $g^*=1.7$. Not treated data of the sample are shown in Fig. 1(d).

in i-$Al_{62}Cu_{25.5}Fe_{12.5}$, we found instead $F_\sigma=1.1$. The last statements here may seen discouraging, but we believe that the true F_σ must be close to $F_{\sigma\text{-max}}$ as when the assumption of a saturated or almost saturated WL effect can be justified (see below).

For "low" fields the theories give $\Delta\sigma(B,T)$ $=-\alpha'(T)B^2$. This simplifies a fit by a separation of the B and T dependences. In practice this gives about the same result as fitting $\Delta\sigma(B)/\sigma \leq 1\%$ for all T, but it is simpler and the strength of the T dependence of $\Delta\sigma(B)$ can be displayed visually. In Figs. 4(a)–4(c), we show $\alpha'(T)$ for i-$Al_{62.5}Cu_{25}Fe_{12.5}$, i-$Al_{62}Cu_{25.5}Fe_{12.5}$, i-$Al_{62.8}Cu_{26}Fe_{11.2}$, R-$Al_{62.8}Cu_{26}Fe_{11.2}$, i-$Al_{70.5}Pd_{22}Mn_{7.5}$, and α-$Al_{72.5}Mn_{17.4}Si_{10.1}$. The $\alpha'(T)$ values span over about five orders of magnitude for each sample, with the magnitude in $\alpha'(T)$ decreasing very fast above 50 K. There is a saturation tendency for $\alpha'(T)$ at low T. The small T dependence we observe below 1 K can be explained by the EEI effect. Thus, the assumptions of a saturated WL effect can be justified. Also, the strength of the T dependence increases with increasing T. In Figs. 4(a)–4(c), we have indicated two straight lines and their power laws, but this is only a guide for the eye. However, in i- and R-$Al_{62.8}Cu_{26}Fe_{11.2}$ [Fig. 4(a)] as well as in α-$Al_{72.5}Mn_{17.4}Si_{10.1}$ [Fig. 4(c)], there seems to be a single power-law behavior over almost two orders of magnitude in T. Finally, around 100 K or higher, we observe a change of sign in $\alpha'(T)$ for most of the samples. In Figs. 4(a)–4(c) the points with a negative $\alpha'(T)$, i.e., positive magnetoconductance, are indicated by filled symbols. The approximate temperatures for this change of sign are tabulated in Table I.

The theoretical expressions for QI in the "low-" field limit are[38]

$$\alpha'(T)=\alpha'_{WL}(T)+\alpha'_{EEI}(T) , \qquad (16)$$

where

$$\alpha'_{WL}(T)=\frac{e^4}{2\pi^2\hbar^3}(D'_{WL}\tau_{so})^{3/2}f(t) , \qquad (17)$$

with

$$f(t)=\frac{1}{96}[t^{-3/2}-3(t+1)^{-3/2}]+\frac{\gamma'}{8}[t^{-1/2}+(t+1)^{-1/2}]$$

$$+\frac{\gamma'}{2}[t^{1/2}-(t+1)^{1/2}] , \qquad (18)$$

$$\gamma'=\left[\frac{g^*\mu_B}{2eD'_{WL}}\right]^2 , \qquad (19)$$

and t is as previously defined and

$$\alpha'_{EEI}(T)=0.056F_\sigma\frac{e^2}{4\pi^2\hbar}(2\hbar D'_{EEI})^{-1/2}(g^*\mu_B)^2(k_BT)^{-3/2} . \qquad (20)$$
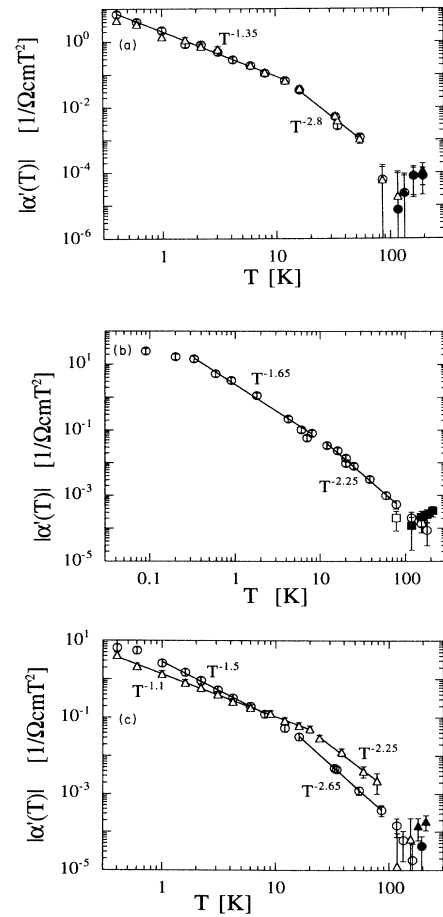
FIG. 4. (a) The absolute value of $\alpha'(T)$ vs temperature (T), with i-$Al_{62.8}Cu_{26}Fe_{11.2}$: $\triangle$ and R-$Al_{62.8}Cu_{26}Fe_{11.2}$: $\bigcirc$. Open symbols are $\alpha'(T)$ positive and filled negative. The $\alpha'(T)$ is defined through $\Delta\sigma(B)=-\alpha'(T)B^2$. The straight lines indicate only the strength of the T dependence, as given beside. A continuous change to a saturation value at the lowest T is more probable. Close to the change of sign in $\alpha'(T)$ the T dependence appears very strong, as given by theory. (b) The absolute value of $\alpha'(T)$ vs temperature (T), with i-$Al_{62}Cu_{25.5}Fe_{12.5}$: $\bigcirc$ and i-$Al_{62.5}Cu_{25}Fe_{12.5}$: $\triangle$. Open symbols are $\alpha'(T)$ positive and filled negative. See also text a. (c) The absolute value of $\alpha'(T)$ vs temperature (T), with i-$Al_{70.5}Pd_{22}Mn_{7.5}$: $\bigcirc$ and α-$Al_{72.5}Mn_{17.4}Si_{10.1}$: $\triangle$. Open symbols are $\alpha'(T)$ positive and filled negative.
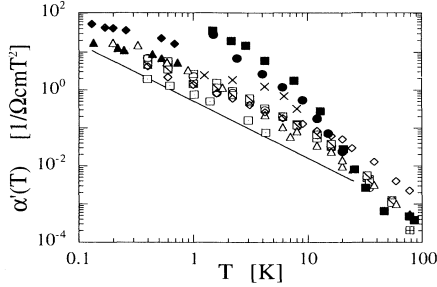
FIG. 5. The absolute value of $\alpha'(T)$ vs temperature. Open symbols define samples presented in this work as follows: i-$Al_{62.8}Cu_{26}Fe_{11.2}$: $\boxminus$; R-$Al_{62.8}Cu_{26}Fe_{11.2}$: $\bigcirc$; i-$Al_{62}Cu_{25.5}Fe_{12.5}$: $\triangle$; i-$Al_{62.5}Cu_{25}Fe_{12.5}$: $\boxplus$; i-$Al_{70.5}Pd_{22}Mn_{7.5}$: $\square$; α-$Al_{72.5}Mn_{17.4}Si_{10.1}$: $\Diamond$; and i-$Al_{70.5}Pd_{22}Re_{7.5}$: $\boxdot$. Filled symbols and crosses define amorphous systems as follows. $Cu_{65}Ti_{35}$ (Ref. 38): $\blacksquare$; $Ni_{35}Ti_{65}$ (Ref. 42): $\bullet$; $Y_{80}Si_{20}$ (Ref. 39): $\blacklozenge$; $Cu_{50}Y_{50}$ (Ref. 39): $\blacktriangle$; $Cu_{50}Lu_0$ (Ref. 39): $\times$. The straight line gives the EEI contribution with $D'_{EEI} = 0.1$ cm^2/s, $g^* = 2$, and $F_\sigma = 1$.

For amorphous metals one may set in many cases $\alpha'_{EEI}(T) \approx 0$. Here, F_σ is larger and D smaller. Further the α's are also smaller than in the metallic glasses (see Fig. 5). The straight line gives $\alpha'(T)_{EEI}$ as calculated from theory with typical values of $D'_{EEI} = 0.1$ cm^2/s, $g^* = 2$, and $F_\sigma = 1$ for QC. The $\alpha'_{EEI}(T) \sim T^{-3/2}$. We understand now that $\alpha'(T)$ may be dominated by EEI contributions at low T and at high T. However, there is a T range, about 1 to 30 K, where the $\alpha'_{EEI}(T)$ only shift $\alpha'(T)$ curves slightly (Figs. 4 and 5). As $T \to 0$, since $\tau_{ie}(T) \sim T^{-p}$, we have $\alpha'_{WL}(T) \sim (\tau_{ie}(T))^{3/2} \sim T^{-3p/2}$. But at other temperatures a simple dependence of $\alpha'_{WL}(T)$ on $\tau_{ie}(T)$ or T is less obvious. We may also have several competing processes in $\tau_{ie}(T)$. This gives $1/\tau_{ie}(T) = \Sigma 1/\tau_n(T)$, where n stands for the different inelastic processes.

We can now get $\tau_{ie}(T)$ from a given value of D'_{WL}, D'_{EEI}, g^*, τ_{so}, and F_σ. We used $D_{Exp}(100$ K$) \leq D'_{WL} \leq D_{Exp}(300$ K$)$ and $1 < g^* < 3$. The latter reflecting the uncertainty in g^* as found in the previous fit of EEI effects. The influence of the EEI part has been diminished by fitting only data in the range 1 to 30 K. The τ_{so} value can be estimated from the size of the positive $\Delta\sigma(B)$. We get $\tau_{so} > 1$ ps, while a direct fit to Eq. (2) with $\Delta\sigma(B,T)/\sigma \leq 2\%$ gives $0.5 \leq \tau_{so} \leq 10$ ps. So we take $1 \leq \tau_{so} \leq 10$ ps for all samples. We can now calculate all τ_{ie} and fit $1/\tau_{ie}(T) = a_0 + a_2 T^p$ with a minimization of the relative deviations. The constants a_0 and a_1 are very sensitive to input parameters. They are for all samples in the ranges $50 < 1/a_0 < 500$ ps and 10 ps/K$^p < 1/a_1 < 500$ ps/K^p. We find that there is a correlation between a_0 and a_1, with a large a_0 for a large a_1. Values of p ($p \sim 1-1.5$) are given in Table I. By assuming the EEI effect is absent above 30 K, the p values only change slightly when the fits are extended to 200 K.

IV. DISCUSSION

In all the investigated quantities such as $\sigma(4.2$ K$)$, $\sigma(T)$, $\Delta\sigma(B)$, $\Delta\sigma(B)/\sigma$, and $\alpha'(T)$, the i- and R-

$Al_{62.8}Cu_{26}Fe_{11.2}$ phases are almost identical [see Figs. 1(a)–1(b) and 4(a)] and similar to the other quasicrystalline system. This is a strong indication because the electron transport is mainly controlled by parameters dominated by the mean range structural order. For R–Al-Cu-Fe the unit cell is large, it is then more surprising that the smaller cubic α-Al-Mn-Si exhibits almost the same transport properties. In the following the i phase and the approximant will not be distinguished.

The electronic screening parameter (F_σ) is enhanced over the values found for amorphous metals. We have $0 \leq F_\sigma \leq 0.5$ for the latter as compared to $F_{\sigma\text{-max}} \geq 0.5$ for the samples studied here. Similar high values have been reported for high structural quality QC previously.[19-21,40] In the Thomas-Fermi approximation and a nearly free-electron model for F_σ, we get an increasing F_σ with decreasing $N(0)/(m^*)^2$. In this model, the highest value is $F_\sigma = 1$ but with the renormalization formula for the screening parameter by Isawa and Fukuyama,[41] we get the maximum value as $F_\sigma = 1.55$. The enhancement of F_σ over values for metallic glasses is thus in accordance with a low $N(0)$ and it favors a $m^* > m_e$ for QC. This also agrees with the results from calculations on approximant models giving many flat bands,[13] which would imply a low electron velocity and a large electron mass. Finally, it has been argued that F_σ may be renormalized as λF_σ with $\lambda > 1$ as for doped semiconductors, where a band-structure effect may enhance F_σ.[6] As far as the g^* are concerned, the g^* values found give no definite answer as to whether g^* is enhanced over or depressed below the free-electron value.

We now compare the high- and low-field temperature dependence of QC and the approximants to that of amorphous metals. Comparing with amorphous metals, the QC and approximants show the larger $\Delta\sigma(B)$ at high fields, thus emphasizing the enhancement of EEI in these systems (see Table I). For the low-field data, the situation is reversed. The values of $\alpha'(T)$ for metallic glasses can differ a factor 10 or more from one system to the other. The QC values are smaller or in the lower range of $\alpha'(T)$ values for amorphous metals, with values for $\tau_{ie}(T)$ and τ_{so} of similar magnitude for both systems.[38,39] Below a few Kelvin, we have a similar T dependence of $\alpha'(T)$ in QC as in metallic glasses and we speculate that the controlling process for $\tau_{ie}(T)$ is the same. However, above about 5 K, the QC have the same T dependence as at lower T, while in amorphous metals $\alpha'(T)$ can be $\sim T^4$ or even stronger.[38,42] A $\tau_{ie}(T)$ term with $p = 3$ or 4 is found,[38,43,44] which is absent for QC and approximants.

The temperature exponent p for the possible scattering mechanisms is for "dirty" ($\tau_{ie} \gg \tau$) systems, $p = 1$,[45] 1.5,[45,46] or 2 (Ref. 46) for the inelastic electron-electron process and $p = 2$,[47] 3,[48] or 4 (Ref. 48) for electron-phonon scattering. In "clean" systems ($\tau_{ie} \approx \tau$), we should have $p = 2$ for the electron-electron scattering, while the electron-phonon part is given by the Bloch-Grüneisen formula. In any case, at high T, we expect electron-phonon scattering to take over with an exponent $p = 1$.

From the values of p obtained, $1.0 \leq p \leq 1.5$ when $1 \leq T \leq 30$ K we conclude that the scattering process in

QC and the approximants is dominated by inelastic electron-electron scattering in the "dirty" limit, and that there is no clear evidence for an electron-phonon scattering term. The same scattering mechanism is expected to dominate in the amorphous metals at low T. The electron-electron scattering with an exponent 1 or 1.5 is expected to be important when D, or $k_F l$, becomes small. For estimating the size of τ_{ie}, we take $\sigma = 150$ $(\Omega \text{ cm})^{-1}$ and $D = 0.1$ cm^2/s as typical QC values and use the nearly free-electron model to estimate $E_F = 2(m_e/m^*)^3$ eV and $\tau = 4 \times 10^{-17}$ $(m^*/m_e)^4$ s. The scattering times in Ref. 45 and 46 becomes now $1/\tau_{ie} \approx 1 \times 10^{13} T (m_e/m^*)^2 + 7 \times 10^{10} T^{3/2}$ 1/s and $1/\tau_{ie} \approx 3 \times 10^9 T^{3/2} + 2 \times 10^6 T^2 (m^*/m_e)^3$ 1/s, respectively. The t term in Ref. 45 seems very small with $m^* = m_e$ and is only reasonable when taking $m^* \geq 20$ m_e. The $T^{3/2}$ terms are of the same magnitude as the $\tau_{ie}(T)$ that we observe, although $7 \times 10^{10} T^{3/2}$ is slightly too small.

The saturation value of τ_{ie} $(1/a_0)$ is of the order of 50 to 500 ps. This is most likely due to magnetic impurities. An inclusion of spin scattering affects on the one hand, the τ_{ie} observed.[24] In thin film experiments on MgCo, Peters, Bergmann, and Mueller[49] found that a Kondo system gives a $\tau_s \sim T^{-1/2}$ dependence in WL below the spin freezing temperature. The spin scattering time τ_s was found to be of the order 20 ps for an impurity concentration of 0.007 atomic layer of Co on Mg. In $Al_{70.5}Pd_{22}Mn_{7.5}$, we estimate $\tau_s \approx 70$ ps within the Born approximation in zero field (assuming spin $S = 2.5$ and the exchange integral $J = 0.25$ eV), with 50 ppm magnetic Mn estimated for our $Al_{70.5}Pd_{22}Mn_{7.5}$ sample by magnetization measurements.[34] Thus, the magnitude of $1/a_0$ is about right. The τ_s may be shorter in $Al_{72.5}Mn_{17.4}Si_{10.1}$ (slightly paramagnetic[34]), but it is definitely longer in the other nonmagnetic samples.[6] Unfortunately, the uncertainty in $1/a_0$ does not allow us to distinguish the weakly magnetic alloys from the nonmagnetic ones.

The spin scattering reduces the WL contribution for low-impurity spin concentration. However, when the concentration is sufficiently high, the WL contribution is enhanced over the value without spin scattering.[50] In this case, a positive magnetoconductance from "classic" Kondo mechanisms is usually present as in $(Y_{1-x}Dy_x)Ni$ amorphous alloys $(x > 0.03)$ found by Amaral *et al.*[51] For our Al-Pd-Mn and Al-Mn-Si alloys, there is only a very small amount of magnetic moments present.[34] A possible magnetic contribution to $\Delta\sigma(B)$ due to these moments must be small, since there is no evident difference between these systems and the other alloys studied here. Chernikov *et al.*[40] studied an $Al_{70}Pd_{21}Mn_9$ sample with $\Delta\sigma(B)$ definitely > 0. This sample exhibited a magnetization corresponding to 1.2% of all Mn atoms (1100 ppm magnetic impurities).[52] In this context, the difficulty that the authors had to explain $\Delta\sigma(B)$ within the simple QI effects is thus natural. A paper on the influence of magnetic impurities on the transport properties in the Al-Pd-Mn system, for samples containing a higher concentration of Mn than studied here, is in preparation.[53]

So far, QI phenomena have been used to explain the $\sigma(T)$ and $\Delta\sigma(B)$ at low temperatures. One may also ask to which extent these effects are present at much higher temperatures. This question is of fundamental interest for explaining the $\sigma(T)$ up to room temperature in not only QC but also amorphous metals. We have seen that the QI theory can explain the behavior of $\Delta\sigma(B)$ for the investigated systems; thus QI effects seems to be present at 200 K. However, there is still no definite answer to the question of whether QI can explain $\sigma(T)$ up to room temperature. The fits give $\Delta\sigma_{WL}(T)$ up to 100 K to be at most 30 $(\Omega \text{ cm})^{-1}$, which would account for most of the conductivity change in QC in this T range; however, for higher temperatures the estimates of $\tau_{ie}(T)$ become very uncertain. Also, the large increase of $\sigma(T)$ at temperatures up to 1000 K, definitely needs another explanation.[10]

An interesting question we have not mentioned so far is as follows: what happens with the QI effects close to the metal-insulator transition (MIT)? The systems that we have studied here have very low conductivities. But we have seen that the $\Delta\sigma(B)$ are of the same magnitude in QC and in metallic glasses; any effect due to the proximity to a MIT does not seem easy to observe. However, in the Al-Pd-Mn system it is possible to obtain a pure QC phase directly by melt spinning and it can be perfected by heat treatment. In Fig. 6, we show the $\Delta\sigma(B)/\sigma$ for as quenched and annealed $Al_{70.5}Pd_{22}Mn_{7.5}$ samples. As can be seen, the $\Delta\sigma(B)/\sigma$ is almost the same, but $\sigma(4.2 \text{ K})$ is 100 and 160 $(\Omega \text{ cm})^{-1}$ for annealed and as quenched, respectively. The $\Delta\sigma(B)$ is thus much smaller in the annealed, i.e., less conducting, sample. This is contrary to what we expect. The $\Delta\sigma(B)$ should increase with decreasing σ, since then either D decreases or $N(0)$ is reduced causing an F_σ enhancement. We have checked to see if this discrepancy can be explained by a small quantity of a second phase of maximally 1–2%, which is the resolution of the X-ray-diffraction experiment. Standard two phase models[54] were used assuming that the second phase has a conductivity of about 10 000 $(\Omega \text{ cm})^{-1}$ and a magnetoconductance $\leq 0.1\%$, but these cannot explain the experimental observations. We thus assume that the change in $\Delta\sigma(B)$ is due to the proximity of the MIT. Recently, $\Delta\sigma(B)/\sigma$ for $Al_{70}Pd_{20}Re_{10}$ was published by Akiyama *et al.*[55] They showed that $\Delta\sigma(B)/\sigma$ was about 3% independent of T for 10 T and $T \leq 1$ K for a sample with $\sigma(4 \text{ K}) \approx 9$ $(\Omega \text{ cm})^{-1}$. First, the T independence indicates
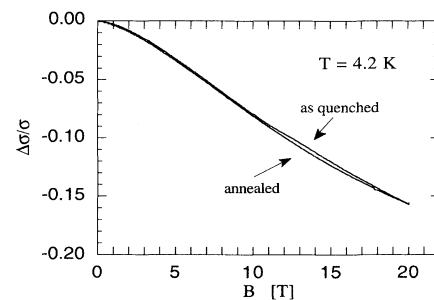
FIG. 6. The $\Delta\sigma(B)/\sigma$ vs B for as quenched and annealed i-$Al_{70.5}Pd_{22}Mn_{7.5}$.

that the EEI effect is absent. This may be due to strong spin-orbit scattering as found in the CaAl amorphous systems when Ag and Au are added,[56] and thus $\Delta\sigma(B)/\sigma$ is due to WL. Second, $\Delta\sigma(10\text{ T}, 0.6\text{ K}) \approx 0.3$ $(\Omega\text{ cm})^{-1}$. This is more than 30 times lower than the values in Table I. Therefore here, also the WL part is strongly suppressed. Values of $\sigma(4\text{ K}) \approx 1$ $(\Omega\text{ cm})^{-1}$, very close to the MIT, have been reported by Pierce, Poon, and Guo[5] in the same system. The tendency here would suggest that $\Delta\sigma(B)/\sigma$ is even smaller for this sample. In Al-Cu-Fe we have $N(0)$ nearly constant, independent of composition. This means that the electrons become increasingly localized as σ and the electronic diffusion constant D tend to zero. The disappearance of $\Delta\sigma(B)$ close to the MIT may be explained as a vanishing probability to perform a closed loop within the lifetime of the coherence length of the electron wave. Further work on this interesting problem is needed.

V. SUMMARY

The magnetoconductance of several quasicrystals and approximant alloys has been studied over a large temperature range and in high magnetic fields. All observed phenomena agree well with different features of quantum interference (QI) effects. This include a larger $\Delta\sigma(B)$, of several percent, which vanishes with increasing temperature. For lower temperatures $\Delta\sigma(B)$ is negative but above 100–200 K it becomes positive. We showed that special care must be taken, concerning the input parameters to the theory, when evaluating the microscopic electronic properties. The analysis showed an enhanced electron-electron interaction in both the weak localization as well as in the electron-electron interaction (EEI) parts to QI. The $\Delta\sigma(B,T)$ is dominated by EEI when $B/T \gg 1$. It is expected that this contribution increases when D decreases, but the enhancement is also due to a enhanced F_σ, with $F_{\sigma\text{-max}} \geq 0.5$. The inelastic scattering time $\tau_{ie} \sim T^{-p}$, with $1.0 \leq p \leq 1.5$, is typical for inelastic electron-electron scattering in a system with $\tau \ll \tau_{ie}$. Both effects are expected in systems where $N(0)$ and D are low. There are strong similarities in the magnitude of the contributions and parameters found here with those in amorphous metals. The only principal differences are the magnitudes of F_σ and the absence of a pronounced inelastic-electron-phonon contribution to $\tau_{ie}(T)$ (of the order $\sim T^{-3}$ or stronger) in the QC and the approximants. The reason why QI theory seems to work so well must be sought in the universal characteristics of QI effects.

[*]Present address: Dept. of Solid State Physics, The Royal Institute of Technology, 100 44 Stockholm, Sweden.

[1]A. P. Tsai, A. Inoe, and T. Masumoto, Mat. Trans. JIM **30**, 666 (1989).

[2]A. P. Tsai, Y. Yoshihiko, A. Inoe, and T. Masumoto, Jpn. J. Appl. Phys. **29**, L1161 (1990).

[3]See, for instance, P. A. Bancel, in *Quasicrystals: The State of the Art*, edited by D. P. Di Vincenzo and P. Steinhart (World Scientific, Singapore, 1991), p. 17.

[4]For a review, see S. J. Poon, Adv. Phys. **41**, 303 (1992).

[5]F. S. Pierce, S. J. Poon, and Q. Guo, Science **261**, 737 (1993).

[6]T. Klein, C. Berger, D. Mayou, and F. Cyrot-Lackmann, Phys. Rev. Lett. **66**, 2907 (1991).

[7]S. Takeuchi, H. Akiyama, N. Naito, T. Shibuya, T. Hashimoto, K. Edagawa, and K. Kimura, J. Non-Cryst. Solids **153 & 154**, 353 (1993).

[8]P. Lanco, T. Klein, C. Berger, F. Cyrot-Lackmann, G. Fourcaudot, and A. Sulpice, Europhys. Lett. **18**, 227 (1992).

[9]B. D. Biggs, S. J. Poon, and N. R. Munirathnam, Phys. Rev. Lett. **65**, 2700 (1990).

[10]D. Mayou, C. Berger, T. Klein, and F. Cyrot-Lackmann, Phys. Rev. Lett. **70**, 3915 (1993).

[11]E. Belin, Z. Dankhazi, A. Sadoc, Y. Calvayrac, T. Klein, and J. M. Dubois, J. Phys. Condens. Matter **4**, 4459 (1992).

[12]A. Katz and M. Duneau, J. Phys. (Paris) **47**, 181 (1986); D. Gratias, Y. Calvayrac, J. Devaud-Repski, F. Faudot, M. Harmelin, and A. Quivy, J. Non-Cryst. Solids **153&154**, 482 (1993).

[13]For a review, see, T. Fujiwara and H. Tsunetsugu, in *Quasi-crystals: The State of The Art* (Ref. 3), p. 343.

[14]M. Cooper and K. Robinson, Acta Crystallogr. **20**, 614 (1966).

[15]F. S. Pierce, P. A. Bancel, B. D. Biggs, O. Guo, and S. J. Poon, Phys. Rev. B **47**, 5670 (1993).

[16]B. D. Biggs, F. S. Pierce, and S. J. Poon, Europhys. Lett. **19**, 415 (1992).

[17]C. Berger, C. Gignoux, O. Tjernberg, P. Lindqvist, F. Cyrot-Lackmann, and Y. Calvayrac, Physica B **204**, 44 (1994).

[18]P. Lindqvist, P. Lanco, C. Berger, G. Foucaudot, A. G. M. Jansen, and F. Cyrot-Lackmann, Physica **194-196**, 399 (1994).

[19]R. Haberkern, G. Fritsch, and J. Schilling, Z. Phys. B **92**, 383 (1993).

[20]A. Sahnoune, J. O. Ström-Olsen, and A. Zaluska, Phys. Rev. B **46**, 10 629 (1992).

[21]T. Klein, H. Rakoto, C. Berger, G. Fourcaudot, and F. Cyrot-Lackmann, Phys. Rev. B **45**, 2046 (1992).

[22]R. Haberkern, P. Lindqvist, and G. Fritsch, J. Non-Cryst. Solids **153&154**, 303 (1993).

[23]B. L. Altshuler and A. G. Aronov, in *Electron-Electron Interaction in Disordered Systems*, edited by A. L. Efros and M. Pollak (North-Holland, Amsterdam, 1985), p. 1.

[24]P. A. Lee and T. V. Ramakrishnan, Rev. Mod. Phys. **57**, 287 (1985).

[25]H. Fukuyama and K. Hoshino, J. Phys. Soc. Jpn. **50**, 2131 (1981).

[26]B. L. Altshuler, D. Khmelnitzki, A. I. Larkin, and P. A. Lee, Phys. Rev. B **22**, 5142 (1980); B. L. Altshuler and A. G. Aronov, Solid State Commun. **46**, 429 (1983).

[27]B. L. Altshuler and A. G. Aronov, Zh. Eskp. Teor. Fiz. **77**,

2028 (1979) [Sov. Phys. JETP **50**, 968 (1979)].

[28]P. A. Lee and T. V. Ramakrishnan, Phys. Rev. B **26**, 4009 (1982).

[29]P. Lindqvist and Ö. Rapp, J. Phys. F **18**, 1979 (1988).

[30]J. C. Ousset, S. Askenazy, H. Rakoto, and J. M. Broto, J. Phys. **46**, 2145 (1985).

[31]V. E. Egoauskin and N. V. Melmikova, J. Phys. F **17**, 1379 (1987).

[32]M. L. Trudeau and R. W. Cochrane, Phys. Rev. B **38**, 5353 (1988).

[33]Ö. Rapp, L. Hedman, T. Klein, and G. Fourcaudot, Solid State Commun. **87**, 143 (1993).

[34]A. Sulpice and J. J. Préjean (unpublished).

[35]C. Berger, T. Grenet, P. Lindqvist, P. Lanco, J. C. Grieco, G. Fourcaudot, and F. Cyrot-Lackmann, Solid State Commun. **87**, 977 (1993).

[36]B. L. Brand, L. G. Rubin, and H. H. Sample, Rev. Sci. Instrum. **59**, 642 (1988).

[37]P. Lindqvist, C. Berger, T. Klein, P. Lanco, and F. Cyrot-Lackmann, Phys. Rev. B **48**, 630 (1993).

[38]P. Lindqvist, J. Phys. Condens. Matter **4**, 177 (1992).

[39]J. B. Bieri, A. Fert, G. Creuzet, and A. Schuhl, J. Phys. Condens. Matter **16**, 2099 (1986).

[40]M. A. Chernikov, A. Bernasconi, C. Beeli, and H. R. Ott, Europhys. Lett. **21**, 767 (1993).

[41]Y. Isawa and H. Fukuyama, J. Phys. Soc. Jpn. **53**, 1415 (1984).

[42]P. Lindqvist, A. Kempf, and G. Fritsch, Z. Phys. B **88**, 159 (1992).

[43]M. A. Howson and B. L. Gallagher, Phys. Rep. **170**, 265 (1988).

[44]C. Von Haesendonk, J. Vranken, and Y. Bruynseraede, Phys. Rev. Lett. **58**, 1968 (1987).

[45]Y. Isawa, J. Phys. Soc. Jpn. **53**, 2865 (1984).

[46]A. Schmid, Z. Phys. **271**, 251 (1974).

[47]B. Keck and A. Schmid, J. Low Temp. Phys. **24**, 611 (1976).

[48]A. Schmid, Z. Phys. **259**, 421 (1973).

[49]R. P. Peters, G. Bergmann and R. M. Mueller, Phys. Rev. Lett. **60**, 1093 (1988).

[50]V. S. Amaral, J. Phys. Condens. Matter **2**, 8201 (1990).

[51]V. S. Amaral, B. Barbara, J. S. Sousa, J. Filippi, A. G. M. Jansen, and J. M. Moreira, Europhys. Lett. **21**, 61 (1993).

[52]M. A. Chernikov, A. Bernasconi, C. Beeli, A. Schilling, and H. R. Ott, Phys. Rev. B **48**, 3058 (1993).

[53]P. Lanco, P. Lindqvist, C. Berger, and F. Cyrot-Lackmann (unpublished).

[54]P. L. Rossiter, *The Electrical Resistivity of Metals and Alloys* (Cambridge University Press, Cambridge, England, 1987).

[55]H. Akiyama, Y. Honda, T. Hashimot, K. Edagawa, and S. Takeushi, Jpn. J. Appl. Phys. **32**, L1003 (1993).

[56]A. Sahnoune, J. O. Ström-Olsen, and H. E. Fischer, Phys. Rev. B **46**, 10035 (1992).